Journal of Mines, Metals and Fuels, *71(12C) : 125-133; 2023. DOI: 10.18311/jmmf/2023/47256*

Print ISSN : 0022-2755

Journal of Mines, Metals and Fuels

Contents available at: *www.informaticsjournals.com/index.php/jmmf*

Linear Stability Analyses of Rayleigh-Benard Convection due to Ternary Hybrid Nanofluid

Mohammed Ayesha[1*] and B. Mallikarjuna[2]

[1]Department of Mathematics, St. Joseph's University, Bengaluru – 560027, Karnataka, India; mdssjasmine@gmail.com
[2]Department of Mathematics, BMS College of Engineering, Bengaluru – 560019, Karnataka, India

Abstract

We aim to study, the linear stability analyses of Rayleigh-Bénard convection in a horizontal layer of ternary hybrid nanofluids. The difficulties concerning the two nano fluid yielded eigen values, which were subsequently obtained and compared. Models of the thermophysical characteristics of nano liquids have been developed based on the characteristics of water as the base liquid and the nanoparticles of aluminum oxide, zirconium oxide, and magnesium oxide. An analytical solution is found for the stationary basic solution of the vertical throughflow. It turns out that the fundamental fields of temperature and velocity are independent of the Newtonian. An examination of linear stability is performed, which results in an eigenvalue problem with order four. The neutral stability curves and the critical Rayleigh number for the onset of instability are obtained by applying a numerical solution to the eigenvalue problem. A strong agreement is discovered when the water results are compared to the findings of earlier studies as a limiting case. A graphic is used to represent the outcomes. The neutral stability curve's location and the critical Rayleigh number are affected by these factors. The different cases of mono, hybrid, and ternary nanofluids are discussed in detail.

Keywords: *Rayleigh-Bénard Convection, Numerical Method, Ternary Hybrid Nanofluid*

1.0 Introduction

A change in the temperature or solute concentration of a fluid changes its local density. This causes a change in buoyancy, resulting in the fluid to move. This particular flow of the fluid is called convection and it is the most commonly seen flow in nature. Heat transfer and mass transfer are also commonly seen in nature and are closely related to people's daily lives and production processes. The most fundamental model for examining the workings of thermal convection is Rayleigh Bernard convection, which is frequently observed in a wide range of natural processes. The use of this mechanism is in the field of geophysics, astrophysics, heat exchangers, meteorology, electronic cooling components and the multilayer walls in buildings etc., Shruthy and Mahanthesh[1] investigated analytically the thermal effect of the Rayleigh Bénard convection in two different fluids namely Casson fluid and hybrid nanofluid. Basak *et al.*[2] looked into the Rayleigh-Benard convection for the zero-magnetic-Prandtl-number fluids and the effect of a uniform vertical magnetic field considering stress-free top and bottom surfaces using direct numerical simulations. Corcione[3] determined that the suspension including nanoparticles is more stable than the pure base liquid; moreover, the degree of stability increases with an increase in both the nanoparticles volume fraction and the average temperature of the nanofluid, and is inversely related to the size of the suspended nanoparticles. In Parsazadeh and Duan[4]'s paper, Aluminium oxide nanoparticles in an enclosure is heated from the bottom using coconut oil as the base phase change material, causing the creation

**Author for correspondence*

of Rayleigh Bénard convection. This was investigated and adding nanoparticles to the melting rate was systematically studied. Reiter *et al.*[5] studied by using direct numerical simulations the effect of heat transport in two and three-dimensional Rayleigh Bénard convection has been analysed with the effects of different thermal sidewall boundary conditions on the formation of flow states. Requile *et al.*[6] discussed the viscous dissipation flow of Rayleigh-Bénard-Couette and Rayleigh-Bénard-Poiseuille through a linear stability analysis. Ouertatani *et al.*[7] studied a classical Rayleigh Bénard convection problem with the numerical method based on the finite volume method and full multigrid acceleration.

Hybrid nanofluids exhibit remarkable thermal behavior and thermophysical features that set them apart from regular fluids. Hybrid nanofluids consist of a blend of two distinct nanoparticles inside a fundamental fluid. Many academics suggested that traditional coolants, particularly those that function at high temperatures, may take the role of hybrid nanofluids. As a result, these nanofluids have a lower negative effect on the environment and save energy. Puneeth *et al.*[8] analysed numerically the unequal diffusion coefficients of bulk fluid and the catalyst within the boundary layer flow of Silver, titanium oxide and water hybrid nanofluid past a thin needle. Nayan *et al.*[9] investigated through a porous medium over a vertical plate the numerically aligned magnetohydrodynamics flow of a hybrid nanofluid. Mallikarjuna *et al.*[10] applied the spectral method in a stretched non-uniform channel with suspended Cu-nanoparticles in different base fluids to study the heat enhancement of nanofluid flow. Kalyan *et al.* [11] analysed the second-order slip conditions for a hydrodynamic nanofluid in a stretchable walled channel and to compute the solutions, the runge-kutta fourth-order based shooting method is used. Kapen *et al.*[12] demonstrated two parallel and stationary plates filled with a porous medium and then studied the flow of a hybrid nanofluid between them and analysed its stability. Alhowaity *et al.*[13] inspected that in the base fluid ethylene glycol if we disperse copper and grapheme nano particles it significantly improves velocity and heat conduction rate over a stretching surface. Redouane *et al.*[14] by using a stable magnetic field, the natural convective heat transfer within a porous triangular cavity filled with a hybrid nanofluid of silver, magnesium oxide, and water was examined. Nadeem *et al.*[15] was analyzed by considering hybrid nanofluids comprising Alumina and Copper nanoparticles within the Sodium Alginate as a host fluid for boosting the heat transfer rate. Manjunatha *et al.*[16] explored the impact of a magnetic field on a tri-hybrid nanofluid that passes through a stretched sheet. Mallikarjuna *et al.*[17] examined the variations in temperature and velocity slip caused by thermal radiation on radiative hydromagnetic two-phase flow via an asymmetric divergence and the governing non-linear differential equation was solved using the shooting technique. To analyze the numerous slip effects on MHD Casson fluid, a mathematical model in a channel with stretchy walls was utilized[18]. The shooting method was utilized to convert and solve the governing equations numerically. Mallikarjuna *et al.*[19] considers the slip effects on MHD micropolar fluid structure in a channel whose walls have been stretched. By using the shooting method, the non-dimensional governing equations have computed.

In modern research, the suspension of three distinct types of nanoparticles in one base fluid is referred to as "ternary hybrid nanofluids". The promising heat transfer rate in multiple scientific disciplines is revealed by thermal investigation of the newly generated ternary hybrid nanofluids with differently shaped nanoparticles. Sneha *et al.*[20] explored the erratic motion of a couple stress via a ternary hybrid nanofluid on a stretched surface with porous media.

An analysis of a one-dimensional dynamic system's stability around its equilibrium points is called a linearized stability analysis. Knowledge regarding the rate at which adjacent trajectories approach or depart from equilibrium or fixed locations may be obtained through the investigation of linearized stability. Pudhir *et al.*[21] examined the linear stability of a fluid layer containing nanoparticles in the presence of a solute gradient. Masuda and Tagawa[22] examined the natural convection of a liquid metal in the presence of a toroidal static magnetic field within an annular container with a square cross section. The linearized disturbance equations in the cylindrical coordinate system are found by applying the finite difference approach. The stability of the Rayleigh-Bénard convection system in a horizontal layer of water-alloy and water-copper nanoliquids was investigated by Veena and Siddheshwar[23]. Dhananjay *et al.*[24] used the Galerkin-type weighted residuals method for the stability analysis after examining the Rayleigh Bernard instability for nanofluid. Roy and Murthy[25] observed a notable viscous dissipation, on the thermo-

solutal convection for both negative and positive Soret parameters. Pourjafar *et al.*[26] rheopectic fluids' linear stability was examined using the Quemada model, and the numerically iterative shooting scheme approach was applied to examine the Couette flow via a poro-elastic layer. Barletta *et al.*[27] used stability analysis to explain the instability for a power law non-Newtonian fluid resulting from through flow convection in a vertical manner across a horizontal saturated porous layer. Adachi *et al.*[28] Application of the linear stability theory to the complicated laminar flow through the spectral element approach is studied in relation to the extended eigenvalue problem related to matrix form. Zainal *et al.*[29] examined the magnetohydrodynamic flow of the hybrid nanofluid, which consisted of copper and aluminum oxide, over a sheet that was stretching and contracting due to quadratic velocity features in the stability context. Barletta *et al.*[30] analytically found the result of the linear equations for the perturbation wave using the power series method and by a fourth-order Runge-Kutta method found the solution numerically. Dhananjay *et al.*[31] used the Galerkin-type weighted residuals method for the stability analysis after examining the Rayleigh Bernard instability for nanofluid.

2.0 Mathematical Formulation

We have considered a laminar incompressible ternary hybrid nanofluid between the horizontal channels. In compared to the top surface temperature T_0, the bottom surface $T_0 + \Delta T$ is kept at a greater temperature. The horizontal walls are towards the x-axis and the vertical walls are towards the y-axis and z-axis.The base fluid H_2O is mixed with the nanoparticles Al_2O_3, ZrO_2 and MgO to create ternary hybrid nanofluid (Figure 1).

2.1 The Governing Equations

Conservation of mass

$$\nabla \cdot \vec{q} = 0 \tag{1}$$

Conservation of linear momentum

$$\rho_{Tnf}\left[\frac{\partial \vec{q}}{\partial t} + (\vec{q}.\nabla)\vec{q}\right] = -\nabla p + \left[\rho_{Tnf}(T_0) - (\rho\beta)_{Tnf}(T - T_0)\right]\vec{g} + \mu_{Tnf}\nabla^2\vec{q}. \tag{2}$$

Conservation of energy

$$\frac{\partial T}{\partial t} + (\vec{q}.\nabla)T = \alpha_{Tnf}\nabla^2 T. \tag{3}$$

Boundary conditions are given by

$$\left.\begin{aligned} T = T_0 \quad \text{at} \quad z = \frac{h}{2} \\ T = T_0 + \Delta T \ \text{ at } \ z = -\frac{h}{2} \end{aligned}\right\} \tag{4}$$

2.2 Thermo-physical and Rheological Properties

The thermophysical properties of Al_2O_3 - ZrO_2 - MgO - H_2O ternary hybrid nanofluid are

$$\mu_{Tnf} = \frac{\mu_f}{(1-\phi_1)^{2.5}(1-\phi_2)^{2.5}(1-\phi_3)^{2.5}}$$

(Brinkman model1952),

$$\kappa_{Tnf} = \left[\frac{\kappa_1 + 2\kappa_{hnf} - 2\phi_1(\kappa_{hnf} - \kappa_1)}{\kappa_1 + 2\kappa_{hnf} + \phi_1(\kappa_{hnf} - \kappa_1)}\right]\left[\frac{\kappa_2 + 2\kappa_{nf} - 2\phi_2(\kappa_{nf} - \kappa_2)}{\kappa_2 + 2\kappa_{nf} + \phi_2(\kappa_{nf} - \kappa_2)}\right]\left[\frac{\kappa_3 + 2\kappa_f - 2\phi_3(\kappa_f - \kappa_3)}{\kappa_3 + 2\kappa_f + \phi_3(\kappa_f - \kappa_3)}\right]\kappa_f$$

(Hamilton Crosser model 1962) ,

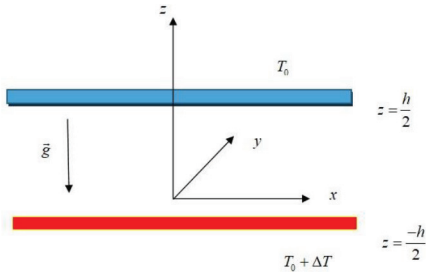


Figure 1. Description of the physical problem.

$$\left.\begin{aligned}
&\alpha_{Tnf}=\frac{\kappa_{Tnf}}{(\rho C_p)_{Tnf}},\\
&\rho_{Tnf}=(1-\phi_1)\left\{(1-\phi_2)\left[\begin{matrix}(1-\phi_3)\rho_f\\+\phi_3\rho_3\end{matrix}\right]+\phi_2\rho_2\right\}+\phi_1\rho_1,\\
&(\rho\beta)_{Tnf}=(1-\phi_1)\left\{\begin{matrix}(1-\phi_2)\left[\begin{matrix}(1-\phi_3)(\rho\beta)_f\\+\phi_3(\rho\beta)_3\end{matrix}\right]\\+\phi_2(\rho\beta)_2\end{matrix}\right\}+\phi_1(\rho\beta)_1,\\
&(\rho C_p)_{Tnf}=(1-\phi_1)\left\{\begin{matrix}(1-\phi_2)\left[\begin{matrix}(1-\phi_3)(\rho C_p)_f\\+\phi_3(\rho C_p)_3\end{matrix}\right]\\+\phi_2(\rho C_p)_2\end{matrix}\right\}+\phi_1(\rho C_p)_1
\end{aligned}\right\}$$

We examine the domains of velocity, pressure, and temperature in a stationary state to be $q_b(z)=(0,0), P=P_b(z)$ and $T=T_b(z)$, which satisfy the following equations:

$$-\nabla P_b=-\left[\rho_{Tnf}(T_0)-(\rho\beta)_{Tnf}(T-T_0)\right]\vec{g}, \tag{5}$$

$$\frac{d^2T_b}{dz^2}=0. \tag{6}$$

The equation (5) is solved for T_b by applying the boundary conditions (4) and we arrive at

$$T_b(z)=T_0+\Delta T\left(\frac{1}{2}-\frac{z}{h}\right). \tag{7}$$

We superpose the motionless state by a small disturbance, in the following form:

$$\vec{q}=\vec{q}_b+\vec{q}';\ T=T_b+T';\ P=P_b+P' \tag{8}$$

In the equations (1)-(3) the values given by equation (8) are substituted, we obtain

$$\begin{aligned}&\rho_{Tnf}\left[\frac{\partial\vec{q}'}{\partial t}+(\vec{q}'.\nabla)\vec{q}'\right]=-\nabla P'\\&+(\rho\beta)_{Tnf}T'\vec{g}\hat{k}+\mu_{Tnf}\nabla^2\vec{q}'\end{aligned} \tag{9}$$

$$\frac{\partial T'}{\partial t}+(\vec{q}'.\nabla)T'-\frac{\Delta T}{h}w'=\alpha_{Tnf}\nabla^2T'. \tag{10}$$

The resulted equations (9) and (10) are non dimensionalized using the definitions given below:

$$\begin{aligned}&\vec{q}=\frac{\vec{q}'h}{\alpha_f},\ P=\frac{h^2P'}{\mu_f\alpha_f},\ (X,Z)=\left(\frac{x}{h},\frac{z}{h}\right),\\&\theta=\frac{T'}{\Delta T'},\ \tau=\frac{t\alpha_f}{h^2},\ w=\frac{hw'}{\alpha_f}.\end{aligned} \tag{11}$$

We obtain the dimensionless equations

$$\frac{A_1}{\mathrm{Pr}_{nf}}\left[\frac{\partial\vec{q}}{\partial\tau}+(\vec{q}.\nabla)\vec{q}\right]=-\nabla P+A_2Ra_c\theta\hat{k}+A_3\nabla^2\vec{q}, \tag{12}$$

$$\frac{\partial\theta}{\partial\tau}+(\vec{q}.\nabla)\theta-w=A_4\nabla^2\theta. \tag{13}$$

Where $\mathrm{Pr}_{nf}=\frac{\mu_f}{\rho_f\alpha_f}$ (Prandtl number for nano liquid),

$Ra_c=\frac{(\rho\beta)_f g\Delta Th^3}{\mu_f\alpha_f}$ (Rayleigh number for nano liquid),

$$A_1=\frac{\rho_{Tnf}}{\rho_f},\ A_2=\frac{(\rho\beta)_{Tnf}}{(\rho\beta)_f},\ A_3=\frac{\mu_{Tnf}}{\mu_f},\ A_4=\frac{\alpha_{Tnf}}{\alpha_f}.$$

2.3 Linear Stability Analysis

The study of linear stability is achieved by neglecting the non-linear term present in the equations. Normal modes technique is used to linearized the above equations (12) and (13), and it's given by

$$\frac{-\nabla P}{A_1}+\frac{A_2}{A_1}Ra_c\theta\hat{k}+\frac{A_3}{A_1}\nabla^2\vec{q}=0, \tag{14}$$

$$\frac{w}{A_4}+\nabla^2\theta=0. \tag{15}$$

Table 1. Thermo-physical properties of the nanoparticles and the base fluid

Quantity	ρ $\left[kg\,m^{-3}\right]$	Cp $\left[J(kg\,K)^{-1}\right]$	κ $\left[W(mK)^{-1}\right]$	β $\left[K^{-1}\right]$
H_2O	997.1	4179	0.6071	21×10^5
Al_2O_3	3970	765	40	0.85×10^5
ZrO_2	5680	502	1.7	0.0005
MgO	3560	955	45	0.0004

Employing curl twice on the equation (14) and considering the Z-component of the resulting equation, we get

$$\frac{A_3}{A_1}\nabla^4 w+\frac{A_3}{A_1}Ra_c\nabla_1^{\,2}\theta=0 \tag{16}$$

The steady-state version is considered since the principle of exchange of stabilities holds in the present problem. The normal mode solution for w and θ is

$$(w,\theta)=\left[W(Z),\Theta(Z)\right]\exp i(\mathrm{K}X), \tag{17}$$

Where W,Θ and K represents the amplitudes of velocity, temperature and the horizontal wave number respectively.

By substituting equation (17) in equations (15) and (16), the following equations are obtained

$$\frac{A_3}{A_1}\left(D^2-\mathrm{K}^2\right)^2 W-\frac{A_2}{A_1}\mathrm{K}^2 Ra_c\Theta=0, \tag{18}$$

$$\frac{W}{A_4}+\left(D^2-K^2\right)\Theta=0, \tag{19}$$

Where $D=\dfrac{d}{dz}$

Using the boundary conditions given below:

At $z=-\dfrac{1}{2}$

$$W=0,\ DW=0,\ \Theta=0. \tag{20}$$

At $$z=\frac{1}{2}$$

$$W=0,\ D^2W=0,\ D\Theta=0. \tag{21}$$

Equations (18) and (19) involving boundary conditions (20) and (21) are numerically solved by the use of the shooting technique, yielding the values of the critical Rayleigh numbers.

3.0 Numerical Procedure

The transformed governing equations (18) and (19) are combined with the boundary conditions (20) and (21) to produce an initial value problem, which is then solved using the shooting approach and the Runge-Kutta fourth order method. The nano particle values are considered from the Table 1.

$$W=f(1);\quad DW=f(2);\quad D^2W=f(3);$$

$$D^3W=f(4);\quad D^4W$$
$$=\frac{A_2}{A_3}\mathrm{K}^2Ra_c\Theta-\mathrm{K}^2W+2\mathrm{K}^2D^2W$$

$$\theta=f(5);\quad D\theta=f(6);$$
$$D^2\theta=K^2\theta-\frac{W}{A_4};\ Ra_c=f(7).$$

Using the above relations, the Equations (18) and (19) are converted to first order equations as follows:

$$\frac{d}{dz}\begin{bmatrix}f(1)\\f(2)\\f(3)\\f(4)\\f(5)\\f(6)\\f(7)\end{bmatrix}=\begin{bmatrix}f(2)\\f(3)\\f(4)\\\frac{A_2}{A_3}\mathrm{K}^2f(7)f(5)-\mathrm{K}^2f(1)+2\mathrm{K}^2f(3)\\f(6)\\\mathrm{K}^2f(5)-\frac{f(1)}{A_4}\\f(7)\end{bmatrix} \tag{22}$$

Equation (22) in vector form $\left[f(1),f(2),f(3),f(4),f(5),f(6),f(7)\right]$ with initial conditions at $f(1),f(2),f(5)$ and $f(7)$. We assume the initial conditions which are not given in (20) and (21) as $f(3)=\alpha_1$, $f(4)=\alpha_2$ and $f(6)=\alpha_3$ are determined by using the shooting technique and integrate equation (22) using Runge-Kutta fourth order method. To verify if the supposed beginning values are accurate, the produced results are compared with the original circumstances. Provide some additional values to the variables that were not provided at the beginning if the difference disappears, and then repeat the previous procedures. In order to get around this, we used the Newton Raphson technique to precisely select the initial conditions and integrated equation (22) using RK4 method with a step size of 0.001 and 106 precision for the solution.

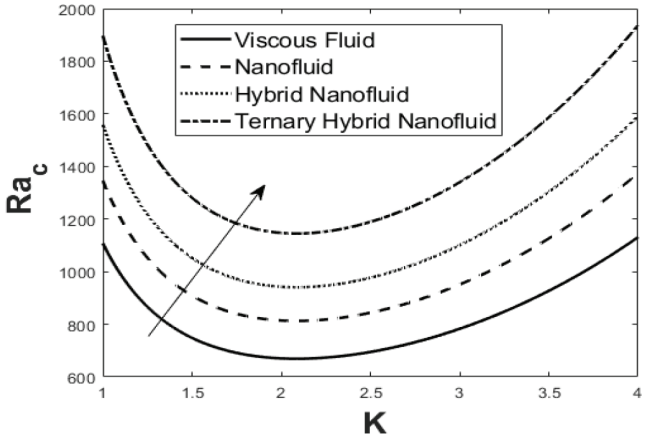


Figure 2. Wave number K versus the Critical Rayleigh number Ra_c for various fluid types.

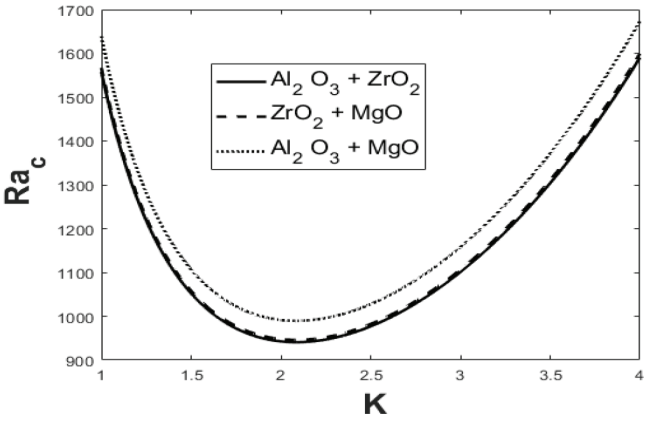


Figure 3. Wave number K versus the Critical Rayleigh number Ra_c for various types of hybrid nanofluids.

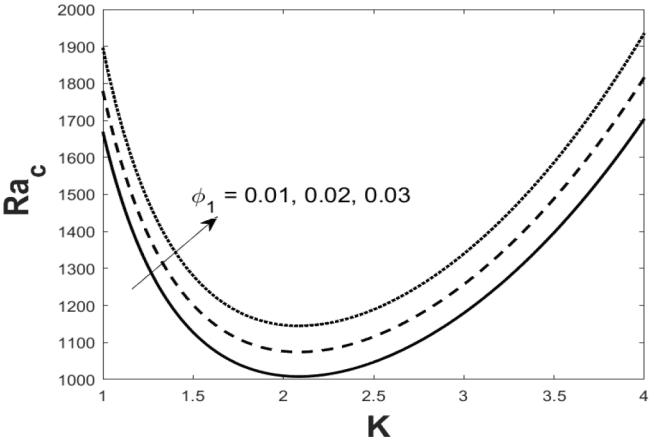


Figure 4. Wave number K versus the Critical Rayleigh number Ra_c with the variation of solid volume fraction ϕ_1 of nanoparticle (Al_2O_3).

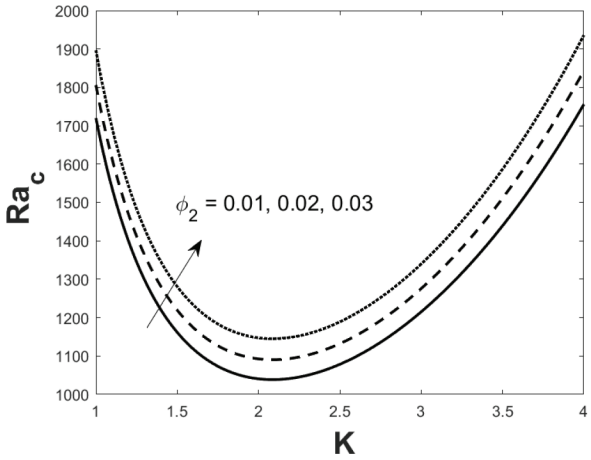


Figure 5. Wave number K versus the Critical Rayleigh number Ra_c with the variation of solid volume fraction ϕ_2 of nanoparticle (ZrO_2).

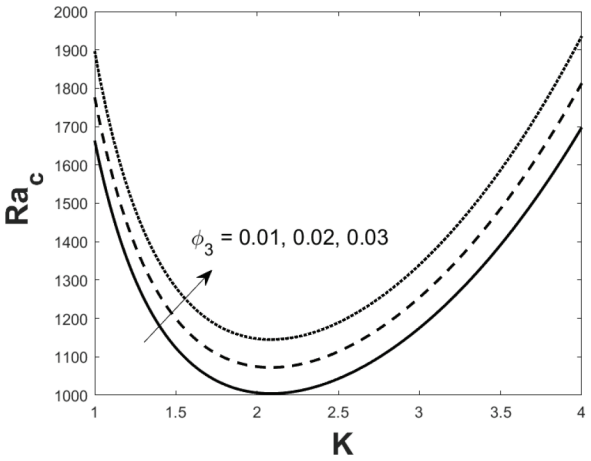


Figure 6. Wave number K versus the Critical Rayleigh number Ra_c with the variation of solid volume fraction ϕ_3 of nanoparticle (MgO).

4.0 Results and Discussions

Using the Runge-Kutta Method and the shooting approach, the dimensionless ordinary differential equation was numerically solved along the boundary conditions specified in (20). We used three distinct kinds of nanoparticles Al_2O_3 - ZrO_2 - MgO in the base fluid H_2O for our research work

Figure 2 illustrates how the heat transfer behavior of viscous fluid, nanofluid, hybrid nanofluid, and ternary hybrid nanofluid may be compared. The ternary hybrid nanofluid is found to have a variety of nanoparticles with

distinct chemical connections, all of which contribute to enhanced heat transmission. This is because each nanoparticle has unique capabilities based on its chemical relationship. Better heat transmission properties are the outcome compared to other fluids. Figure 3 reveals the result on Ra_c with K for different hybrid nanoparticles.

Figures 4-6 reveal the results on Ra_c with K for different values of ϕ. We inspected different values of solid volume fraction for three different nanoparticles namely, aluminium oxide (Al_2O_3), Zirconium oxide (ZrO_2) and Magnesium oxide (MgO) and this indicates that the Critical Rayleigh number Ra_c will rise as the solid volume fraction ϕ of the nanoparticles increases.

5.0 Conclusion

The problem of linear stability analyses of Rayleigh-Bénard convection due to ternary hybrid nanofluids between horizontal plates investigated.

- Basic state solution has been calculated and then governing equations are non dimensionalized.
- Considering Linear terms of the equations and making use of normal modes of unknowns and the resulted equations are solved numerically.
- The governing equations are transformed into ordinary differential equations by using the appropriate transformation. In order to create simultaneous first-order differential equations, the higher-order ordinary differential equations that arise are transformed.
- Runge-Kutta fourth order-based shooting method has been implemented to find the solutions and the results are interpreted through graphs.
- Considered three different nanoparticles Aluminium oxide, Zirconium oxide and Magnesium oxide to investigate its influence on the stability of Rayleigh-Bénard Convection.
- Critical Rayleigh number Ra_c is computed concerning wave number K for different values of solid volume fraction of different nanoparticles.
- When the solid volume fraction is increased the heat capacitance of the nanofluid is improved.
- The ternary hybrid nanofluid has superior heat transfer properties than both the nanofluid and the hybrid nanofluid.
- The ternary hybrid nanofluid has the ability to conduct more heat for a greater solid volume percentage.
- We may conclude from the corresponding studies and graphs that the ternary hybrid nanofluid is far more effective at transferring heat than both the hybrid and the nanofluid.

6.0 References

1. Shruthy M, Mahanthesh B. Rayleigh-Bénard convection in Casson and hybrid nanofluids: An analytical investigation. J Nanofluids. 2019; 8(1):222-9. https://doi.org/10.1166/jon.2019.1571
2. Basak A, Raveendran R, Kumar K. Rayleigh-Bénard convection with uniform vertical magnetic field. 2021.
3. Corcione M. Rayleigh-Bénard convection heat transfer in nanoparticle suspensions. Int J Heat Fluid Flow. 2011; 32(1):65-77. https://doi.org/10.1016/j.ijheatfluidflow.2010.08.004
4. Parsazadeh M, Duan X. Effects of nanoparticles on phase change heat transfer rate in the presence of Rayleigh-Bénard convection. Int J Heat Mass Transf. 2020; 156:119831. https://doi.org/10.1016/j.ijheatmasstransfer.2020.119831
5. Reiter P, Zhang X, Shishkina O. Flow states and heat transport in Rayleigh-Bénard convection with different sidewall boundary conditions. J Fluid Mech. 2022; 936:1-29. https://doi.org/10.1017/jfm.2022.56
6. Requilé Y, Hirata SC, Ouarzazi MN. Viscous dissipation effects on the linear stability of Rayleigh-Bénard-Poiseuille/Couette convection. Int J Heat Mass Transf. 2020; 146. https://doi.org/10.1016/j.ijheatmasstransfer.2019.118834
7. Ouertatani N, Cheikh NB, Beya BB, Lili T. Numerical simulation of two-dimensional Rayleigh-Bénard convection in an enclosure. Comptes Rendus-Mec. 2008; 336(5):464-70. https://doi.org/10.1016/j.crme.2008.02.004
8. Puneeth V, Manjunatha S, Makinde OD, Gireesha BJ. Bioconvection of a radiating hybrid nanofluid past a thin needle in the presence of heterogeneous-homogeneous chemical reaction. J Heat Transfer. 2021; 143(4):1-9. https://doi.org/10.1115/1.4049844
9. Nayan A, Fauzan NIFA, Ilias MR, Zakaria SF, Aznam NHZ. Aligned Magnetohydrodynamics (MHD) flow of hybrid nanofluid over a vertical plate through porous medium. J Adv Res Fluid Mech Therm Sci. 2022; 92(1):51-64. https://doi.org/10.37934/arfmts.92.1.5164
10. Mallikarjuna B, Ramprasad S, Shehzad SA, Ayyaz R. Numerical and regression analysis of Cu-nanoparticles flows in distinct base fluids through a symmetric non-uniform channel. Eur Phys J Spec Top. 2022; 231(3):557-69. https://doi.org/10.1140/epjs/s11734-021-00400-w

11. Chakravarthy YSK, Prasad SR, Mallikarjuna B, Babu RS. Numerical and linear regression analysis of slip effects on Magnetohydrodynamics (MHD) convective Cu-water nanofluid flow in a channel with stretchable walls. J Nanofluids. 2022; 11(4):616-27. https://doi.org/10.1166/jon.2022.1856
12. Kapen PT, Ketchate CGN, Fokwa D, Tchuen G. Linear stability analysis of (Cu-Al_2O_3)/water hybrid nanofluid flow in porous media in presence of hydromagnetic, small suction and injection effects. Alexandria Eng J. 2021; 60(1):1525-36. https://doi.org/10.1016/j.aej.2020.11.007
13. Alhowaity A, Bilal M, Hamam H, Alqarni MM, Mukdasai K, Ali A. Non-Fourier energy transmission in power-law hybrid nanofluid flow over a moving sheet. Sci Rep. 2022; 12:10406. https://doi.org/10.1038/s41598-022-14720-x
14. Redouane F, Jamshed W, Devi SSU, Prakash M, Nasir NAAM, Hammouch Z, *et al*. Heat flow saturate of Ag/MgO-water hybrid nanofluid in heated trigonal enclosure with rotate cylindrical cavity by using Galerkin finite element. Sci Rep. 2022; 12:2302. https://doi.org/10.1038/s41598-022-06134-6
15. Nadeem M, Siddique I, Awrejcewicz J, Bilal M. Numerical analysis of a second-grade fuzzy hybrid nanofluid flow and heat transfer over a permeable stretching/shrinking sheet. Sci Rep. 2022; 12(1). https://doi.org/10.1038/s41598-022-05393-7
16. Manjunatha S, Puneeth V, Gireesha BJ, Chamkha AJ. Theoretical study of convective heat transfer in ternary nanofluid flowing past a stretching sheet. J Appl Comput Mech. 2022; 8(4):1279-86.
17. Mallikarjuna B, Bhatta SHCVS, Ramprasad S. Velocity and thermal slip effects on MHD convective radiative two-phase flows in an asymmetric non-uniform channel. Propuls Power Res. 2021; 10(2):169-79. https://doi.org/10.1016/j.jppr.2021.04.002
18. Mallikarjuna B, Ramprasad S, Chakravarthy YSK. Multiple slip and inspiration effects on hydromagnetic Casson fluid in a channel with stretchable walls. Int J Heat Technol. 2020; 38(4):817-26. https://doi.org/10.18280/ijht.380407
19. Mallikarjuna B, Chakravarthy YSK, Ramprasad S. Effect of multiple forces on convective micropolar fluid flow in a permeable channel with stretching walls considering second order slip conditions. Int J Ambient Energy. 2022; 43(1). https://doi.org/10.1080/01430750.2022.2059004
20. Sneha KN, Vanitha GP, Mahabaleshwar US, Laroze D. Effect of couple stress and mass transpiration on ternary hybrid nanoliquid over a stretching/shrinking sheet with heat transfer. Micromachines. 2022; 13(10):1-24. https://doi.org/10.3390/mi13101694
21. Pundir SK, Awasthi MK, Kumar V. Double-diffusive convection in a hybrid nanofluid layer. J Nanofluids. 2022; 11(2):296-304. https://doi.org/10.1166/jon.2022.1831
22. Masuda T, Tagawa T. Linear stability analysis of three-dimensional natural convection at low Prandtl number in an annular enclosure in the presence of a toroidal magnetic field. AIP Adv. 2020; 10(12). https://doi.org/10.1063/5.0024354
23. Veena BN, Siddheshwar PG. Linear and non-linear stability analyses of Rayleigh-Bénard convection in water-copper and water-alloy nanoliquids. Int J Ambient Energy. 2022; 43(1):7229-36. https://doi.org/10.1080/01430750.2022.2063186
24. Dhananjay Y, Agrawal GS, Bhargava, R. Rayleigh-Bénard Convection in Nanofluid. Int J Appl Math Mech. 2011; 7(2):61-76.
25. Roy K, Murthy PVSN. Linear stability of the double-diffusive convection in a horizontal porous layer with open top: Soret and viscous dissipation effects. Transp Porous Media. 2018; 122(3):693-712. https://doi.org/10.1007/s11242-018-1022-5
26. Pourjafar M, Bazargan S, Sadeghy K. Linear stability analysis of time-dependent fluids in plane Couette flow past a poroelastic layer. J Nonnewton Fluid Mech. 2019; 266:1-19. https://doi.org/10.1016/j.jnnfm.2019.02.003
27. Barletta A, Storesletten L. Linear instability of the vertical throughflow in a horizontal porous layer saturated by a power-law fluid. Int J Heat Mass Transf. 2016; 99:293-302. https://doi.org/10.1016/j.ijheatmasstransfer.2016.03.115
28. Adachi T, Uehara H. Linear stability analysis of flow in a periodically grooved channel. Int J Numer Meth Fluids. 2003; 41:601-13. https://doi.org/10.1002/fld.456
29. Zainal NA, Nazar R, Naganthran K, Pop I. Magnetic impact on the unsteady separated stagnation-point flow of hybrid nanofluid with viscous dissipation and joule heating. Mathematics. 2022; 10(13). https://doi.org/10.3390/math10132356
30. Barletta A, Celli M, Rees DAS. The onset of convection in a porous layer induced by viscous dissipation: A linear stability analysis. Int J Heat Mass Transf. 2009; 52(1-2):337-344. https://doi.org/10.1016/j.ijheatmasstransfer.2008.06.001
31. Pranesh S, Bawa R. Rayleigh-Bénard convection in nanofluid. 2014; 2014(Nield):562106.

Nomenclature

C_p	Specific heat $\left(J\,(kg\,K)^{-1}\right)$
$\vec{g}$	Acceleration due to gravity
$\vec{q}$	Velocity vector
h	Height
κ	Thermal conductivity
K	Wave number
p	Pressure
P	Non-dimensional pressure
T	Temperature
T_0	Temperature at the upper boundary
t	Time
u	Horizontal velocity component (m/s)
w	Vertical velocity component (m/s)
x	Horizontal Cartesian coordinate (m)
X	Non-dimensional horizontal coordinate
z	Vertical Cartesian coordinate (m)
U,W	Non-dimensional versions of the velocity component
Z	Non-dimensional vertical coordinate
R_a	Rayleigh number

Greek symbols

α	Thermal diffusivity
μ	Dynamic viscosity
ρ	Actual density
β	Thermal expansion coefficient
ϕ	Volume fraction
τ	Non-dimensional time
θ,Θ	Non-dimensional temperature

Subscripts

f	Fluid
b	Basic state
c	Critical
nf	Nanofluid
Tnf	Ternary hybrid Nanofluid